Laminar Free Convection In Horizontal Annulus Filled With Glass Beads And With Annular Fins On The Inner Cylinder

Asst. Prof. Dr. Manal Hadi saleh
University of Baghdad
manalhadi2005@yahoo.com

Ahmed Mohsen Katea
University of Baghdad
ahmed_msc2013@yahoo.com

ABSTRACT

An experimental and numerical study has been carried out to investigate the heat transfer by natural convection and radiation in a two dimensional annulus enclosure filled with porous media (glass beads) between two horizontal concentric cylinders. The outer cylinders are of (100, 82 and70mm) outside diameters and the inner cylinder of 27 mm outside diameter with (or without) annular fins attached to it. Under steady state condition; the inner cylinder surface is maintained at a high temperature by applying a uniform heat flux and the outer cylinder surface at a low temperature inside a freezer. The experiments were carried out for an annulus filled with glass beads at a range of modified Rayleigh number ($4.9 \leq Ra \leq 69$), radiation parameter ($0<Rd<10$), with fin length of (Hf=3, 7 and 11mm), with radius ratios of ($Rr=(r_1/r_2)$ =0.1405, 0.2045, 0.293 and 0.3649), number of fins (n=0, 12, 23 and 45). Finite difference method with Boussinesq's approximation is used to solve the continuity, energy and momentum equations. The numerical solution is capable of calculating the streamline, the temperature field, the velocity field, the local and average Nusselt number. A computer program in Mat lab has been built to carry out the numerical solution. The numerical study was done for a range of modified Rayleigh number ($4.9 \leq Ra \leq 300$). Results show that the average Nusselt number is nearly constant for Ra less than 100 and increased with an increase in modified Rayleigh number. Nusselt number hardly affected by glass beads size and insignificant affected by Rd for Ra less than 100. Decreasing Rr cause clearly increase in average Nusselt number and increasing fin length or fin number decrease heat transfer.

KEY WORDS: Laminar, natural convection, radiation, two dimensional, horizontal annulus enclosure, glass beads and annular fins.

الحمل الحر الطباقي في محتوى حلقي افقي مملوء بكرات زجاجية بوجود زعانف متصلة بالأسطوانة الداخلية

الاستاذ المساعد د. منال هادي صالح

المهندس احمد محسن كاطع

الخلاصة:

أجريت في هذا البحث دراسة عملية ونظرية لإنتقال الطاقة الحرارية بالحمل الحر والاشعاع في فجوة حلقية ثنائية الأبعاد مملوءة بوسط مسامي (كرات زجاجية) بين أسطوانتين افقيتين متحدتي المركز بوجود (أو عدم وجود) زعانف متصلة بالإسطوانة الداخلية تحت شروط حالة الإستقرار. حفظ سطح الأسطوانة الداخلية بدرجة حرارية ثابتة وعالية بتسليط فيض حراري منتظم وتم حفظ سطح الأسطوانة الخارجية بدرجة حرارية ثابتة وواطئة داخل حجرة التجميد في ثلاجة. أجريت التجارب العملية على فجوة حلقية مملوءة بوسط مسامي (كرات زجاجية) ولمدى عدد رالي المعدّل (($4.9 \leq Ra \leq 69$) والاشعاع المنتقل ($0<Rd<10$) ولطول زعنفة (Hf =3,7 and 11mm) ونسبة الأقطار (Rr=0.1405,0.2045,0.293, 0.364) ولعدد زعانف (n=12, 23,45). أستخدمت طريقة الفروق المحددة وتقريب بوسنسك لحل معادلة الإستمرارية والطاقة والزخم. تم بناء برنامج بلغة ماتلاب لتنفيذ الحل العددي ومن ثم تمثيل عدد نسلت المتوسط والموقعي ومخططات توزيع درجات الحرارة والسرعة لبيان جريان المائع وانتقال الطاقة الحرارية. أجريت الدراسة العددية لمدى عدد رالي المعدّل ($4.9 \leq Ra \leq 300$). بينت النتائج أن معدل نسلت المتوسط ثابت تقريبا عندما يكون عدد رالي المعدّل أقل من 100 ويزداد عندما يزداد الاخير وان قطر الكرات الزجاجية تأثيرها قليل جدا ويؤثر الاشعاع بمقدار ضئيل عند قيم عدد رالي المعدّل الأقل من 100. وكذلك بينت ان تناقص نسبة الاقطار يزيد من عدد نسلت المتوسط و إن زيادة طول وعدد الزعانف يقلل من انتقال الحرارة.

كلمات رئيسية : طباقي، حمل حر، اشعاع، ثنائي الابعاد، حيز حلقي افقي، كرات زجاجية، زعانف حلقية

INTRODUCTION

Phenomena of natural convection heat transfer in horizontal annuli with or (without) fins and filled with porous media had been studied in many fields due to its more important applications. Natural convection in a cylindrical annulus has attracted much attention in relation to solar collectors, thermal storage systems and spent nuclear fuel cooling while natural convection in porous annuli has a wide variety of technological applications such as the insulation of an aircraft cabin and thermal insulation of buildings or horizontal pipes, reactors, the storage of thermal energy, and underground cable systems, ground water flows oil recovery processes [Nield and Bejan 1999] and [Kumari et al. 2008]. Although the mechanics of the flow in porous media preoccupied engineers and scientist for more than century, the phenomenon of convection heat transfer has achieved the status of separate field of research only during the last four decades [Wajeeh 2006]. An experimental and numerical study had been carried out by [Manal 2011] to investigate the heat transfer by natural convection in a three dimensional annulus enclosure filled with porous media between two inclined concentric cylinders. It was found that the average Nusselt number depends on (Ra, Hf, δ and Rr) and the maximum value of the local Nusselt number for vertical cylinder is about twice as large as that of the horizontal case. The results showed that, increasing of fin length increases the heat transfer rate for any fins pitch unless the area of the inner cylinder exceeds that of the outer one, then the heat will be stored in the porous media. The unsteady natural convection flow from a horizontal cylindrical annulus filled with a non-Darcy porous medium has been studied by [Fukuda et al. 1980] for Grashof numbers of Gr $=3.7\times 10^{3}$ and 5.4×10^{3} and Darcy numbers of Da= 2×10^{-4} and 2×10^{-2}. The unsteadiness in the problem arises due to the impulsive change in the wall temperature of the outer cylinder. The Navier–Stokes equations along with the energy equation governing the unsteady natural convection flow have been solved by the finite-volume method. The results showed that the annulus completely filled with a porous medium has the best insulating effectiveness. In case of annulus partially filled with a porous material, insulating the region near the outer cylinder is more effective than insulating the region near the inner cylinder.

To extend the existing studies, a parametric two dimensional laminar free convection in an horizontal annulus with porous media and with (and without) fins attached to the inner cylinder will be addressed. The experiments were carried out for an annulus filled with glass beads at a range of modified Rayleigh number ($4.9 \leq Ra \leq 69$), radiation parameter ($0<Rd<10$), with fin length of (Hf=3, 7 and 11mm), with radius ratios of ($Rr=(r_1/r_2)$ =0.1405, 0.2045, 0.293 and 0.3649), number of fins (n=0, 12, 23 and 45).

EXPERIMENTAL STUDY

Two outer cylinders of different diameters were manufactured to vary the radius ratio and to vary the fin length; ten inner cylinders were manufactured one without fins and the others with different fin with a specifications shown in **Table 1**. To investigate the effect of the parameters and the effect of modified Rayleigh number by the variation of the temperature difference between the two concentric cylinders by means of a variable electric input power. Aluminum was chosen because of its high thermal conductivity and easy machinability. The test section consists of a two Aluminum outer cylinders of (100 mm) and (82 mm) outside diameters, (4 mm) thick and (260mm) long to which ten Aluminum inner cylinders of (27mm) outside diameter, (260 mm) long and (5 mm) thick. The inner cylinder was heated by passing an alternating current to a heater inside the inner cylinder and the outer cylinder was subjected to the surrounding temperature (freezer) where the minimum temperature was 270 K. The inner cylinder surface temperatures were measured at six locations using thermocouples type (K). The experimental apparatus is shown diagrammatically in Fig. 1

MATHEMATICAL MODEL:

The geometry and coordinate system of the problem considered are illustrated in **Fig. 2**. The heat conducted through the fin heats up the porous medium on the two vertical sides of the fin. Then, due to the heating of the porous medium from the fin, the buoyancy force, which acts vertical upward, causes an upward-directed flow in the porous medium on both sides of the fin. In order to model the incompressible flow in the porous medium, the steady-state equations of the Darcy flow model, namely, the mass, the momentum (Darcy), the energy conservation laws and the Boussinesq's approximation are employed. These equations in vectorial notation are given by **[**Manal 2011**]** as shown in **Fig. 2.**

Assumptions

To obtain a mathematical simulation for the natural convection flow being studied, the following assumptions have been made:

1. The convective fluid remains in a single-phase.
2. Incompressible flow.
3. The porous medium is considered to be homogeneous and isotropic.
4. Flow in the annulus is steady state laminar and two dimension in (r,z) direction assuming long annulus.
5. The density of the fluid assumed constant except when it's happened directly from flotation force **[**Mahony et al. 1986**]** and in buoyancy term (ρ g) depends linearly on temperature.
6. The solid material is non deformable.
7. The convective fluid and the solid are in local thermal equilibrium everywhere.
8. Compression work is negligible.
9. Chemical reactions in the system are negligible.
10. Darcy's law is applicable.
11. The viscous dissipation is neglected because its effect is usually small in laminar free convective flows at ordinary temperatures **[**Gebhart 1963**].**
12. Boundaries are not permeable.

Governing Equations

The conservation equations of mass, momentum and energy in steady state and the supplementary equation are [Fukuda et. al. 1980]:

$$\rho = \rho_2 \{1 - \beta(T - T_2)\} \qquad (1)$$

Where

$$\beta = \frac{1}{\rho}\left(\frac{\partial \rho}{\partial T}\right) \qquad (2)$$

β is the thermal coefficient of the volume expansion; this constant is evaluated at T2 which is the temperature at the inner surface of the outer cylinder, ρ_2 is the density at T_2 and ρ is the density at T, [Fukuda et al. 1980].This technique is called Boussinesq's approximation.

Mass conservation:

$$\frac{1}{r}\frac{\partial}{\partial r}(r v_r) + \frac{\partial v_z}{\partial z} = 0 \qquad (3)$$

Momentum Equation:

$$v_r = -\frac{K}{\mu_f}\left[\frac{\partial p}{\partial r} + g\rho_2\{\beta(T - T_2)\}\right] \text{ in r direction} \qquad (4)$$

$$v_z = -\frac{K}{\mu_f}\left[\frac{\partial p}{\partial z}\right] \text{In z direction} \qquad (5)$$

Energy Equation:

$$v_r\frac{\partial T}{\partial r} + v_z\frac{\partial T}{\partial z} = \alpha[\frac{1}{r}\frac{\partial}{\partial r}(r\frac{\partial T}{\partial r}) + \frac{\partial}{\partial z}\left(\frac{\partial T}{\partial z}\right)$$

$$+\frac{1}{r}\frac{\partial}{\partial r}(\frac{r q_r}{k})] \qquad (6)$$

$$q_r = -\frac{4\sigma\partial T^4}{3\beta\partial r} \qquad (7)$$

$$\alpha = \frac{k}{\rho C_p} \qquad (8)$$

α is convective thermal diffusivity (m^2/s),and q_r is Radiation flux.

Fin Equation:

Within the fin itself, the energy equation is **[**James 1974**]:**

$$\frac{1}{r}\frac{\partial T}{\partial r} + \frac{\partial^2 T}{\partial r^2} + \frac{\partial^2 T}{\partial z^2} = 0 \qquad (9)$$

Dimensionless Governing Equations

The characteristic length for the present study is r_{out} [Manal 2011**]** to convert the governing equations to the dimensionless form; the dimensionless magnitudes must be defined as follow:

$$R = \frac{r}{r_{out}},\ Z = \frac{z}{r_{out}},\ H_1 = \frac{H_f}{r_{out}}$$

$$V_r = \frac{v_r\ l}{\alpha_{eff}},\quad V_z = \frac{v_z\ l}{\alpha_{eff.}},\qquad V_r = -\frac{1}{R}\frac{\partial\Psi}{\partial Z},$$

$$V_z = \frac{1}{R}\frac{\partial\Psi}{\partial R}$$

$$\theta = (T - T_2)/(T_1 - T_2),\ P = \frac{p\ K\ l}{\alpha_{eff}\ \mu_f\ r_{out}},$$

$$Ra = g\ \beta\ K\ (T_1 - T_2)\ (r_{out} - r_{in})/\alpha_{eff.}\ \upsilon$$

Taking curl of momentum equations to eliminate pressure terms, the momentum and the energy equation will be:

$$\left(\frac{\partial^2\Psi}{\partial Z^2}\right) + \left(\frac{\partial^2\Psi}{\partial R^2}\right) - \frac{1}{R}\frac{\partial\Psi}{\partial R}] = Ra\ \frac{-1}{(r_{out}-r_{in})}\frac{\partial\theta}{\partial Z} \tag{10}$$

$$\frac{r_{out}}{l}\left[\frac{\partial\Psi}{\partial R}\frac{\partial\Theta}{\partial Z} - \frac{\partial\Psi}{\partial Z}\frac{\partial\Theta}{\partial R}\right] = \mathrm{R}\,\frac{\partial^2\Theta}{\partial Z^2} + R(1+\frac{4}{3}Rd)\left(\frac{\partial^2\theta}{\partial R^2}\right) + \left(1+\frac{4}{3}Rd\right)\frac{\partial\theta}{\partial R} \tag{11}$$

Where Rd is radiation parameter which can be defined as:

$$\mathrm{Rd} = \frac{4\sigma_i\,\Delta T_\infty^3}{\beta_r k} \tag{12}$$

Dimensionless Fin Equation:

$$\frac{1}{R}\left(\frac{\partial\theta}{\partial R}\right) + \left(\frac{\partial^2\theta}{\partial R^2}\right) + \frac{\partial^2\theta}{\partial Z^2} = 0 \tag{13}$$

Dimensionless Hydraulic Boundary Conditions:

$$\frac{1}{R}\frac{\partial}{\partial R}(R\psi) = 0 \qquad at\ \ R = R_1, 1$$

$$\frac{\partial\psi}{\partial Z} = 0 \qquad at\ \ Z = 0,\ \ L$$

And for the fin, the boundary conditions are given as:

$$\frac{1}{R}\frac{\partial}{\partial\ R}(R\ \psi_r) = \frac{\partial\ \psi_Z}{\partial\ Z} = 0$$

On the fin faces which were located on the following planes:

At R = R_1 for (fin base)

At r = r_1+Hf for (fin tip)

As shown in **Fig. 3**

Dimensionless Thermal Boundary Conditions:

$$\theta = 1 \qquad at\ \ R = R_1 = r_{in}/r_{out}$$

$$\theta = 0 \qquad at\ \ R = R_2 = 1$$

$$\frac{\partial\theta}{\partial Z} = 0 \qquad at\ \ Z = 0,\ \ L$$

$$-k_{fin}\frac{\partial\theta}{\partial R}\Big|_{fin} = -k_{eff.}\frac{\partial\theta}{\partial R}\Big|_{medium}\ at\ \ R = H_1$$

$$-k_{fin}\frac{\partial\theta}{\partial Z}\Big|_{fin} = -k_{eff.}\frac{\partial\theta}{\partial Z}\Big|_{medium} \qquad at\ S_1\ \ for\ any\ R$$

$$and\ at\ S_2 \qquad for\ any\ R$$

keff. =the effective thermal conductivity

of the medium (W/mK).

$$\mathrm{K_{eff}} = (1-\varepsilon)\ \mathrm{k_s} + \varepsilon\ \mathrm{k_f} \tag{14}$$

Fin Efficiency:

The ratio of actual heat transfer from an extended surface to the maximum possible heat transfer (heat which would be transferred if entire fin area were at base temperature) is designated fin efficiency, symbolized η_f and given as **[**James 1974**]:**

$$\eta_f = \frac{1}{1 + \frac{m^2}{3}\sqrt{\frac{d_f}{d_o}}} \qquad (15)$$

$$m = H_f \sqrt{\frac{2h_i}{kt}} \qquad (16)$$

Computational Technique

Eqs.(10, 11and 13) were transformed into the finite difference equations, where the upwind differential method in the left hand side of the energy Eq. (11) and the centered – space differential method for the other terms were used, and solved by using (SOR) method [Wang and Zhang 1990]. The following equation illustrates a sample of finite difference equation for a node on the cylinder.

The partial differential equations were finite-differenced using central difference schemes. In form of finite difference approximation momentum equation become:

$$\Psi_{(i,k)} = [\frac{1}{\Delta R^2}\left(\Psi_{(i+1,k)} + \Psi_{(i-1,k)}\right) + \frac{1}{2\Delta R R(i)}\left(\Psi_{(i+1,k)} - \Psi_{(i-1,k)}\right) + \frac{1}{\Delta Z^2}\left[\Psi_{(i,k+1)} + \Psi_{(i,k-1)}\right] + \frac{Ra^*}{2\Delta Z(r_{out} - r_{in})}(\theta_{(i,k+1)} - \theta_{(i,k-1)})]/[\frac{2}{\Delta Z^2} + \frac{2}{\Delta R^2}] \qquad (17)$$

The finite difference equation on a fin tip is as follow:

$$\theta_{(i,k)} = \left[\left(\left(\frac{1}{2\Delta R R(i)}\right)\right)\left(\theta_{(i+1,k)} - \theta_{(i-1,k)}\right) + \frac{1}{\Delta Z^2}\left(\theta_{(i,k+1)} + \theta_{(i,k-1)}\right) + \left(\left(\frac{1}{\Delta R^2}\right)\right)\left(\theta_{(i+1,k)} + \theta_{(i-1,k)}\right)\right] / \left[\frac{2}{\Delta R^2} + \left(\frac{2}{\Delta Z^2}\right)\right] \qquad (18)$$

A computer program was built using mat lab to meet the requirements of the problem. The value of the stream line will be calculated at each node, in which the value of stream line is unknown, the other node will appear in the right hand side of each equation. As an initial value of iteration, zero is chosen for the stream line field, while a conduction solution is adopted for fins. The index (n) was used to represent the nth approximation of temperature denoted by Θ^n and substituted into the approximated equations, which were solved to obtain the nth –approximation of stream line Ψ, then Ψ was substituted into Eq. (11) to obtain Θ^{n+1}. A similar procedure is repeated until the prescribed convergence criterion given by inequality:

$$Max\left|\frac{\theta^{n+1} - \theta^n}{\theta^n}\right| \le 10^{-8}$$

was established [Fukuda et al. 1980].

As the steps of iteration increase with Ra, a solution obtained for lower Ra was used as an initial value of computation for higher Ra (double iteration method). It is clear that as the grid becomes finer, the convergence of the results becomes better. The number of grid points used was 41 grid points in the R–direction and 401 in the Z – direction which seems reasonable and will be used in the present study. Fig.4 illustrates the numerical grid in two planes.

Calculation of Local and Average Nusselt Number

Nusselt number is the dimensionless parameter indicative of the rate of energy convection from a surface and can be obtained as follows [Fukuda et. al.1980]:

$$Nu = \frac{q\ (r_{out} - r_{in})}{k\ (T_1 - T_2)} \qquad (19)$$

As the local heat flux on the wall is given by:

$$q = -k\frac{\partial T}{\partial r} \qquad (20)$$

The local Nusselt number *Nu1* and *Nu2* on the inner and the outer cylinders are written in the form **[**Fukuda et. al. 1980**]:**

$$Nu_1 = -(1-R_1)\left(\frac{\partial \theta}{\partial R}\right)_{R=R1} \qquad (21)$$

$$Nu_2 = -(1-R_1)\left(\frac{\partial \theta}{\partial R}\right)_{R=1} \qquad (22)$$

The average Nusselt number Nu_{in} and Nu_{out} on the inner and the outer cylinders are defined as:

$$Nu_{in} = -(1-R_1)\left(1+\frac{4}{3}Rd\right)\int_0^L \left(\frac{\partial \theta}{\partial R}\right)_{R=R1} dZ \qquad (23)$$

$$Nu_{out} = -(1-R_1)\left(1+\frac{4}{3}Rd\right)\int_0^L \left(\frac{\partial \theta}{\partial R}\right)_{R=1} dZ \qquad (24)$$

Results and Discussion

Figs. 5 show the variation of the average Nusselt number on the hot cylinder with Ra for different radius ratios, without and with fins respectively. These figures show that for any radius ratio, the average *Nu* is generally constant for low values of Ra then as Ra reached nearly 100, *Nu* increased with increasing Ra. These values increased as *Rr* decreased due to the enlargement of the gap between the two cylinders this improved that for low values of Ra the heat transferred by conduction and as Ra increased the convection heat transfer would be dominant. These figures show that as *Hf* increases *Nu* decreases and decreasing the pitch (by increasing fin numbers) causes *Nu* to decrease. **Fig. 6** illustrates that the values of the average Nusselt number was low for low radius ratio; then they increased with high intensity as radius ratio increased this because as the annulus gap decreased, the resistance to the circulation motion of the convection cells increased and this lead to slower replacement of the hot air adjacent to the inner surface by the cold air adjacent to the outer surface and these resulted in an increase in the average temperature of the annulus inner surface. Convective heat transfer rate is controlled by three parameters (h, A and ΔT), according to

$$Q = h_i A_{in} (T_1 - T_2) = h_o A_{out}(T_1 - T_2)$$

For the same modified Rayleigh number (i.e. ΔT is constant), dQ/Q=(dA/A)+(dh/h). If the increase in the surface area is more than the decrease in the heat transfer coefficient, the total heat transfer rate will increase, or if the decrease in the heat transfer coefficient is more than the increase in the surface area, the total heat transfer rate will decrease [Harith 2009]. This figure indicates that there is a reduction in the average Nusselt number with increasing Hf from 3mm to 11mm. For the same value of Ra .**Figs. 7** indicate that there is a reduction in the average Nusselt number with increasing the number of fins from n=12(pitch=19.2mm) to n=23(pitch=8.4 mm) and then to n=45(pitch=3mm). The distributions of the local Nusselt number are shown in **Fig.8.** which illustrate that attaching fins to the inner cylinder cause the local Nu to be wavy and the waviness decreased with the increase of fin length. It is clear from this figure that adding the effect of radiation cause to increase Nu significantly .**Fig. 9** illustrates a comparison between the experimental and theoretical results for the variation of the average Nusselt number with modified Rayleigh number for different Rr. The average Nusselt number was nearly constant because of the predominance of conduction mode on heat transfer process. For Ra >100 (in the numerical part) convection became predominant mechanism and the average Nusselt number began to clearly increase. Most of the experimental values were lower than that of the numerical; one of the reasons may be the conduction losses through the sides and hence the absence of perfectly insulated ends boundaries and may be because of the assumptions which had been taken and this is true even for this research or for [Prasad and Kulacki 1985] and [Havstad and Burns 1982].**Fig.10** shows the variation of the average Nusselt number on the hot cylinder with Ra for different radiation parameters, without and with fins and for different radius ratios respectively. Nu increase for hot cylinder about 54.6% as Rd increase from zero to ten and this percentage increase with the increase of fin length to be 88% for fin length equal to 11mm. A comparison for the variation of the average Nusselt number on the inner and outer cylinders with Ra was made with that of [Fukuda et al. 1980] in **Fig. 11** and its clear that Nu is constant for low values of Ra, until Ra equal nearly 100, then Nu will increase with increasing of Ra as presented in this work.**Fig.12** shows the contours of isotherms for different values of Ra, radiation parameter (Rd), radius ratio (Rr), fin length (H_f), fin number (n) and glass beads average diameter (d_g) **Fig.13** shows the Z–component of the streamline, in the (R-Z) plane. Contours of velocity field in the (R-Z) plane in the radial direction of the annulus are illustrated in **Fig. 14** and along the length of the annulus are illustrated in **Fig. 15**.

A flow chart for computer program is shown in **Fig. 16**.

UNCERTAINTY ANALYSIS

The uncertainties of experimental quantities were estimated using the method presented by [Holman, 1971**].** Uncertainty values for the Local Nusselt number on the cold wall was varied from 0.32 to 0.83 %, while the uncertainty values for the modified Rayleigh number was between 1.22 to 2.34 % by applying the following equations.

$$\frac{W_{N\bar{u}}}{Nu_{out}} = \left[\left(\frac{W_I}{I}\right)^2 + \left(\frac{W_V}{V}\right)^2 + \left(\frac{W_K}{k}\right)^2 + \left(\frac{W_{\Delta T}}{\Delta T}\right)^2\right]^{1/2}$$

$$\frac{W_{Ra}}{Ra^*} = \left[\left(\frac{W_{\Delta T}}{\Delta T}\right)^2 + 3\left(\frac{W_T}{T_m}\right)^2 + \left(\frac{W_K}{K}\right)^2 + \left(\frac{W_\delta}{w}\right)^2\right]^{1/2}$$

CONCLUSIONS

The following major conclusions can be drawn from the experimental and numerical study**:**

1- For all parameters, results showed that the average Nu number is nearly constant for low Ra and clearly increased with an increase in modified Rayleigh number. It is hardly affected by d_g and insignificant effect of Rd for low values of Ra.

2- Decreasing Rr cause a clearly decrease in average Nusselt number due to the enlargement in the gap.

3- Adding the effect of radiation cause significant increase in average Nusselt number.

4- Increasing fin length or fin number, cause a decrease in heat transfer because of the hindrance effect of the fins.

5- For heat exchanger the best design is an inner cylinder without fins, but for solar collectors and energy storage system, the best design is to use 45 fins of 11mm length.

REFERENCES

Fukuda K., Takata Y., Hasegawa S., Shimomura H. and Sanokawa K., "Three – Dimensional Natural Convection in a Porous Medium between Concentric Inclined Cylinders", Proc. 19th Natl Heat Transfer Conf., Vol. HTD – 8, pp. 97 – 103, 1980.

Gebhart B., "Effect of Viscous Dissipation in Natural Convection", J. Fluid Mech., Vol. 14, Part 4, pp. 255-232, 1963.

Harith Hussein Hamzah, "An Investigation of Fins Geometry Effects for Laminar Free Convection in Horizontal Annulus with Finned Inner Cylinder", M.Sc. Thesis, University of Baghdad, 2009.

Havstad M.A., Burns P.J.," Convective Heat Transfer in Vertical Cylindrical Annuli Filled with a Porous Medium", Int. J. Heat and Mass Transfer, Vol. 25, No.11, pp. 1755-1766, 1982

Holman J. P., "Experimental Methods for Engineers", 4th edition, McGraw Hill, 1971

James R. Welty, "Engineering Heat Transfer", 1st edition by John Wiley & Sons, 1974.

Kumari M. and. Nathb G., "Unsteady Natural Convection from a Horizontal

Annulus Filled with a Porous Medium", Int. J. of Heat and Mass Transfer, Vol, 51, pp. 5001–5007, 2008.

Manal H. Saleh, "Parametric steady of laminar free convection in inclined porous annulus with fins on the inner cylinder" PhD. Thesis, university of Baghdad, 2011.

Nield D. A. and Bejan A., "Convection in Porous Media", Springer-Verlag, New York, 1999.

Mahony D. N., Kumar R. and Bishop E. H.,"Numerical Investigation of Variable Property Effects on Laminar Natural Convection of Gases between Two Horizontal Concentric Cylinders", ASME J. Heat Transfer, Vol. 108, pp. 783-789, November 1986.

Prasad, V. and Kulacki, F. A., "Natural Convection in Porous Media Bounded by Short Concentric Vertical Cylinders", Transaction of ASME, J. of Heat Transfer , Vol. 107, pp. 147-154, February, 1985.

Wajeeh, K. H.; "Transient Three-Dimensional Natural Convection in Confined Porous Media with Periodic Boundary Conditions", PhD. Thesis, University of Technology, 2006.

Wang Bu – Xuan and Zhang Xing, "Natural Convection in Liquid Saturated Porous Media Between Concentric Inclined Cylinders" Int. J. Heat and Mass Transfer Vol. 33. No 5, pp. 827-833, 1990.

NOMENCLATURE

Latin Symbols

Symbol	Description	Units
A_{in}	The surface area of the inner cylinder	m^2
A_{out}	The surface area of the outer cylinder	m^2
C_p	Specific heat at constant pressure	kJ/kg°C
d_f	Fin diameter	M
d_i	Inner diameter of the inner cylinder	M
d_o	Outer diameter of the inner cylinder	M
dg	Diameter of glass bead	mm
g	Acceleration due to gravity	m/s^2
h_f	Heat transfer coefficient of fluid	$W/m^2 K$
H_f	Fin length	m
h_i	The convection heat transfer coefficient on the inner cylinder (hot surface)	$W/m^2 K$
h_o	The convection heat transfer coefficient on the outer cylinder (cold surface)	$W/m^2 K$
$K_{eff.}$	Effective thermal conductivity of the porous media	W/m K
k_f	Thermal conductivity of the fluid	W/m K
k_s	Thermal conductivity of the solid	W/m K
K	Permeability	m^2
l	Cylinder length	m
Nu_1	Local Nusselt number on the inner cylinder	-
Nu_1	Local Nusselt number on the inner cylinder	-
Nu_2	Local Nusselt number on the outer cylinder	-
t	Fin thickness	m
r	Radial coordinate	m
r_{in}	Radius of the inner cylinder	m
r_{out}	Radius of the outer cylinder	m
Ra	Modified Rayleigh number $Ra=Ra^* Da$	-
Rr	Radius ratio $Rr=r_{in}/r_{out}$	-
Rd	Dimensionless radiation	-
R_1	Dimensionless radius for inner cylinder	-
R_2	Dimensionless radius for outer cylinder	-

s	Fin spacing (fin pitch)	m
T	Temperature	K
v_r	Radial velocity component	m/s
v_z	Axial velocity component	m/s
V_r	Dimensionless velocity component in R -direction	-
Vz	Dimensionless velocity component in Z - direction	-
Z	Dimensionless axial coordinate	-
x,y,z	Cartesian coordinate system	

Greek Letters

Symbol	Description	Units
α	Thermal diffusivity	m^2/s
$\alpha_{eff.}$	Effective thermal conductivity of the porous media	m^2/s
β	Volumetric thermal expansion coefficient	1/K
ε	porosity	-
η_f	Fin efficiency	-
θ	Dimensionless temperature	-
μ_f	Dynamic viscosity of fluid	$N.s/m^2$
ρ_2	Reference density at T_2	kg/m^3
σ	Stefan – Boltzmann constant	$W/m^2 K^4$
ψ	streamline	-
ΔR, ΔZ	Distance between the grid points	-

Table 1 system specifications

Test sections and measuring Systems	Specifications
Fin length	3, 7 and 11mm
Radius ratio Rr= (r_{in}/r_{out})	0.1405, 0.2045, 0.293 and 0.3649
Number of fins	12, 23 and 45
digital thermometer type K	$(-50^{\circ}C)$ to $(750^{\circ}C)$
stabilizer type (DACTRON	(110/220 V) with oscillation of (± 1 %)
variac type (TDGC)	(0 – 250) V
Digital Multimeter	(200 V– 750 V)

Table 2 the percent uncertainties of Nu_{out} and Ra^*

	Result	Value	%Uncertainty
1	Nu_{out}	1.17596	0.83
1	Ra^*	11.652	1.22
2	Nu_{out}	3.071135	0.32
2	Ra^*	0.201	2.34

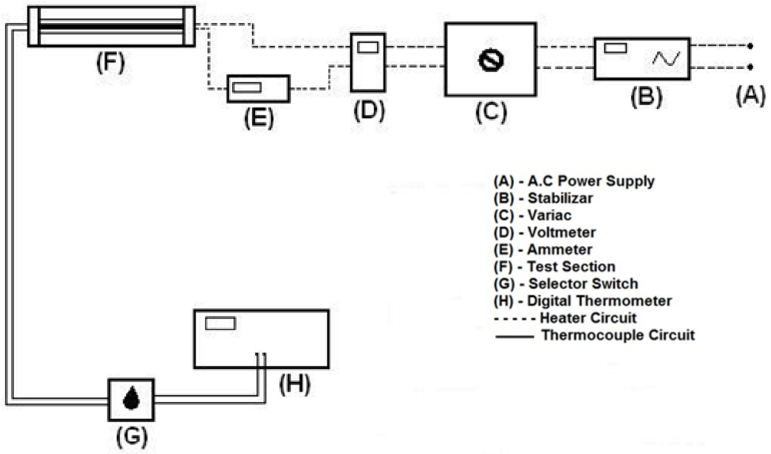

Fig.1 Schematic diagram of experimental apparatus

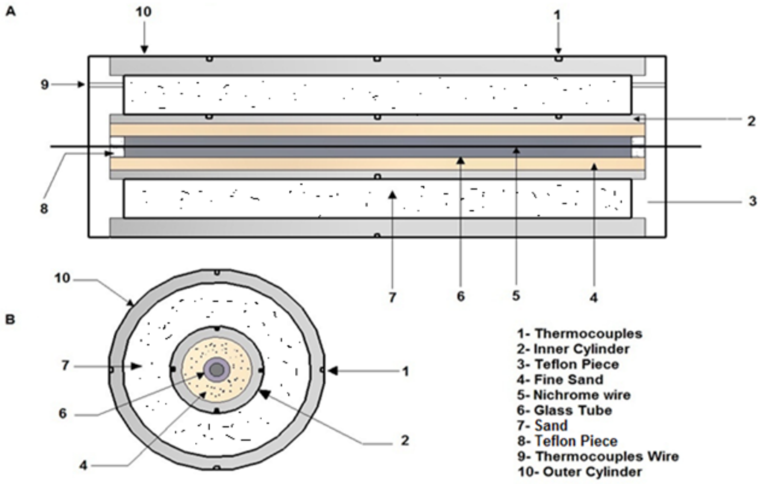

(a)

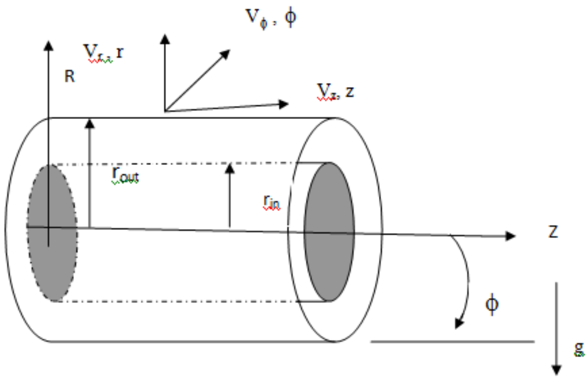

(b)

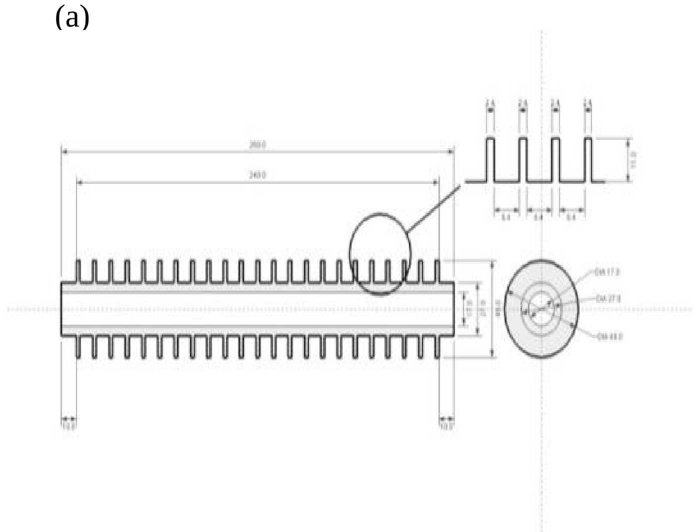

(c)

Fig. 2, (a) Test Section, A- Front View, B- Side View (b) Geometry and coordinates system and (c) Schematic Diagramof Inner Cylinder with n=23

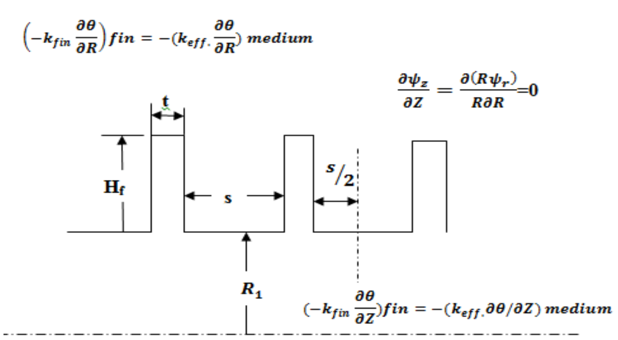

Fig.3. Fin boundary conditions

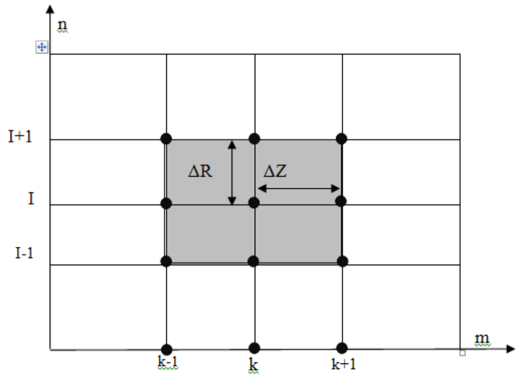

Fig. 4 A plot of two dimensional discretized domain

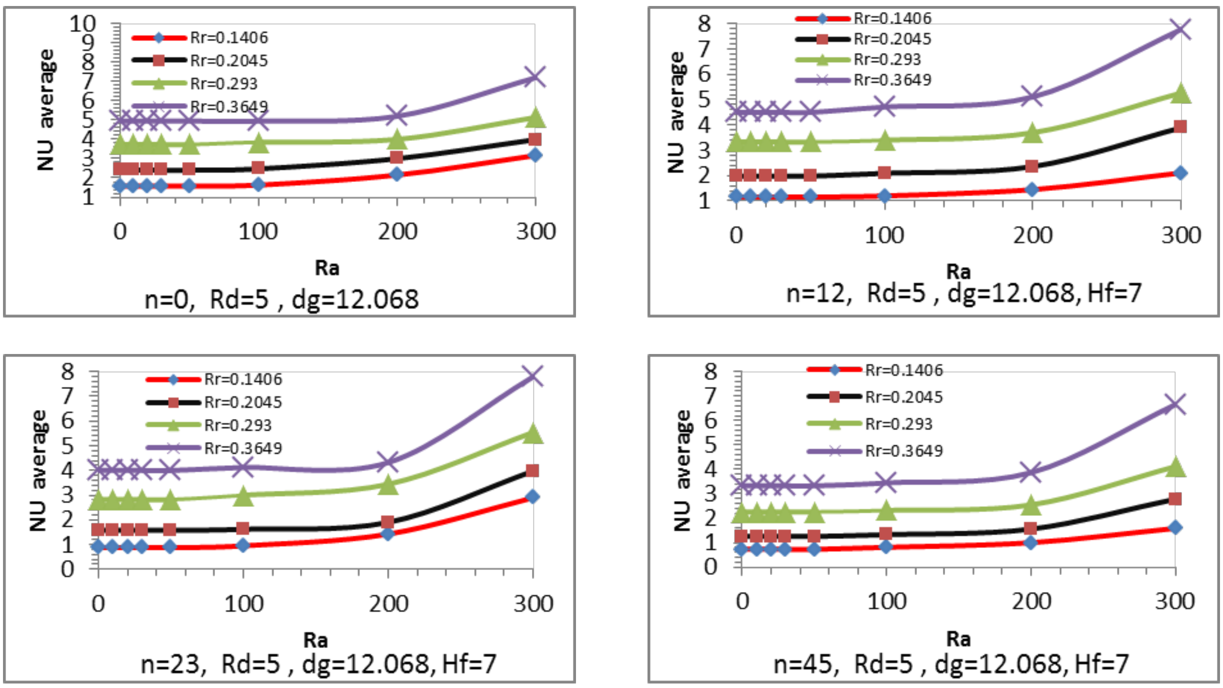

Fig.5 Variation of Average Nu with Ra with different Rr

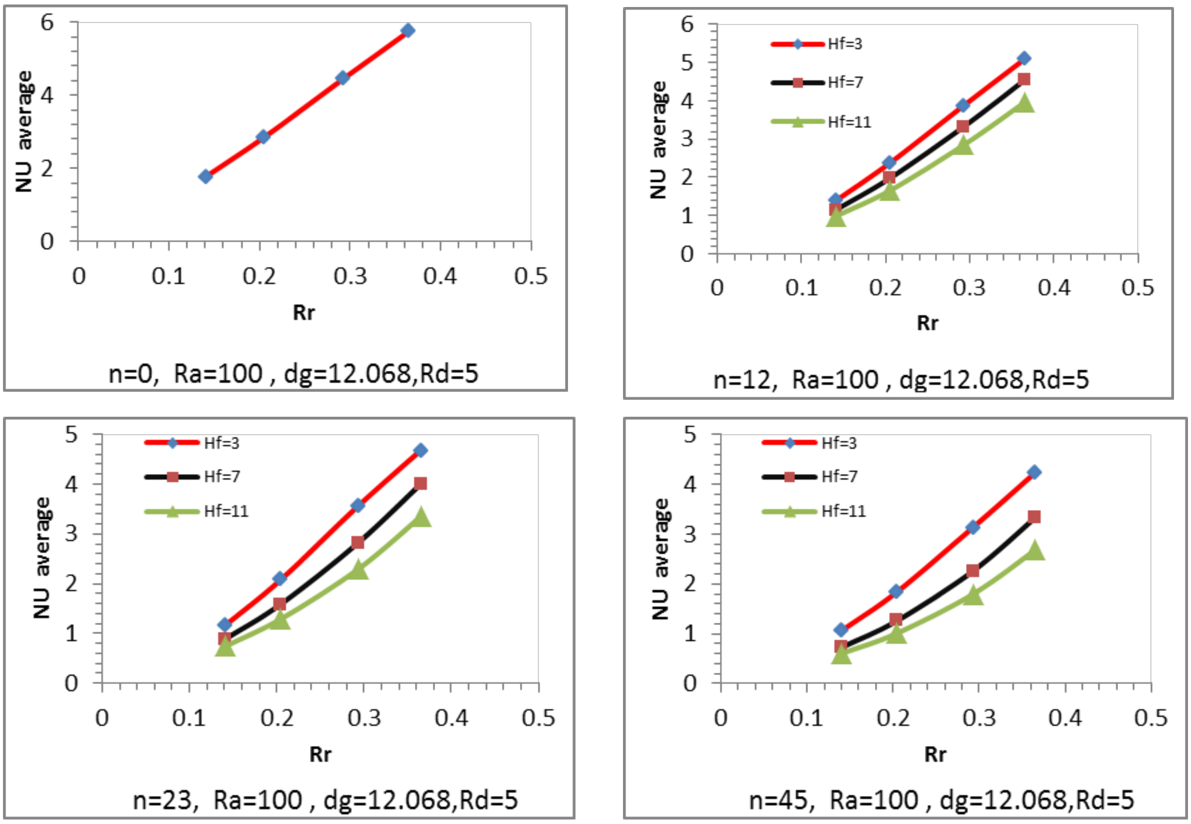

Fig.6 Variation of Average Nu with Rr for different Hf

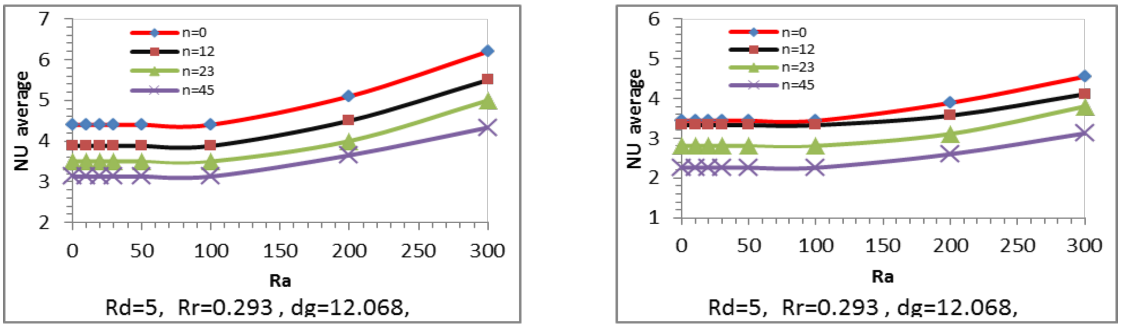

Fig.7 Variation of Average Nu with Ra for different n

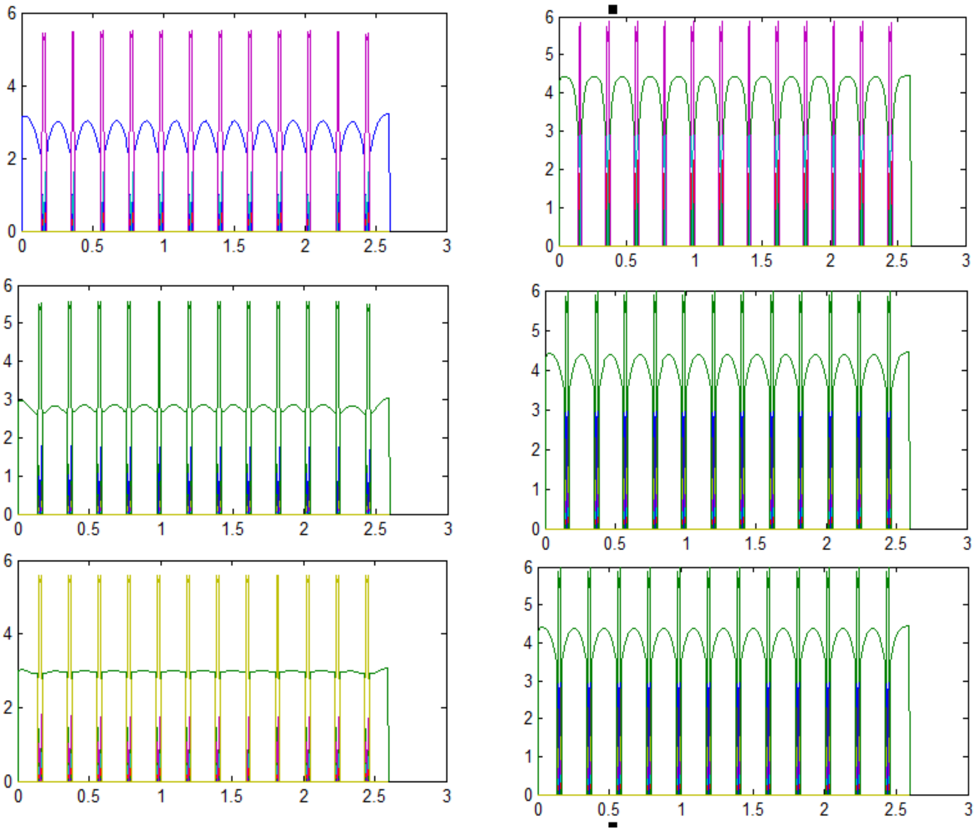

Rd=0 Ra=100 Rr=0.293 d_g=12.068 Hf=3,7,11

Rd=5 Ra=100 Rr=0.293 d_g=12.068 Hf=3,7,11

Fig.8 Variation of local Nusselt number in (Z – Direction) along the hot cylinder wall for (n=12)

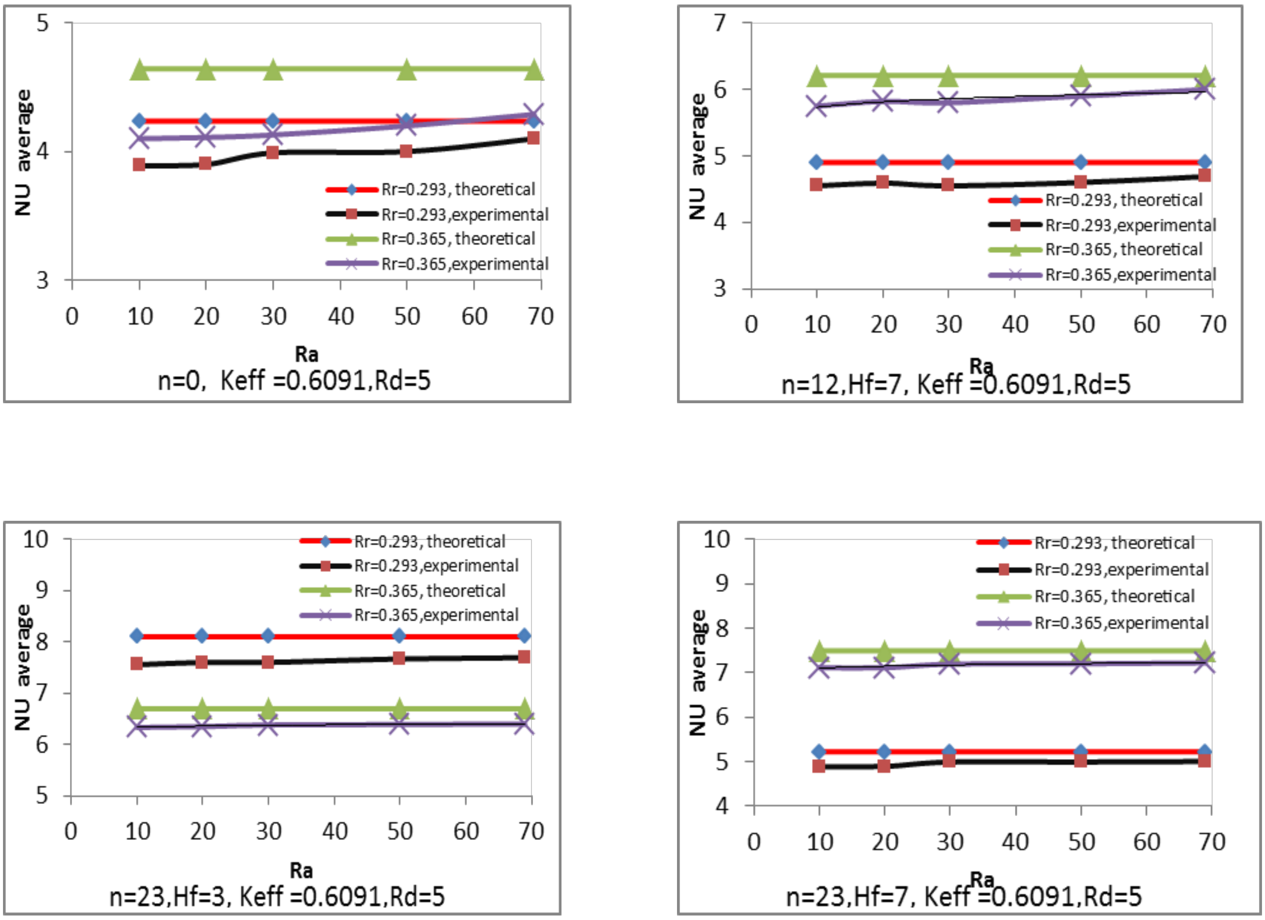

Fig.9 Variation of Average Nusselt Number with Modified Ra for different Rr , n and H_f

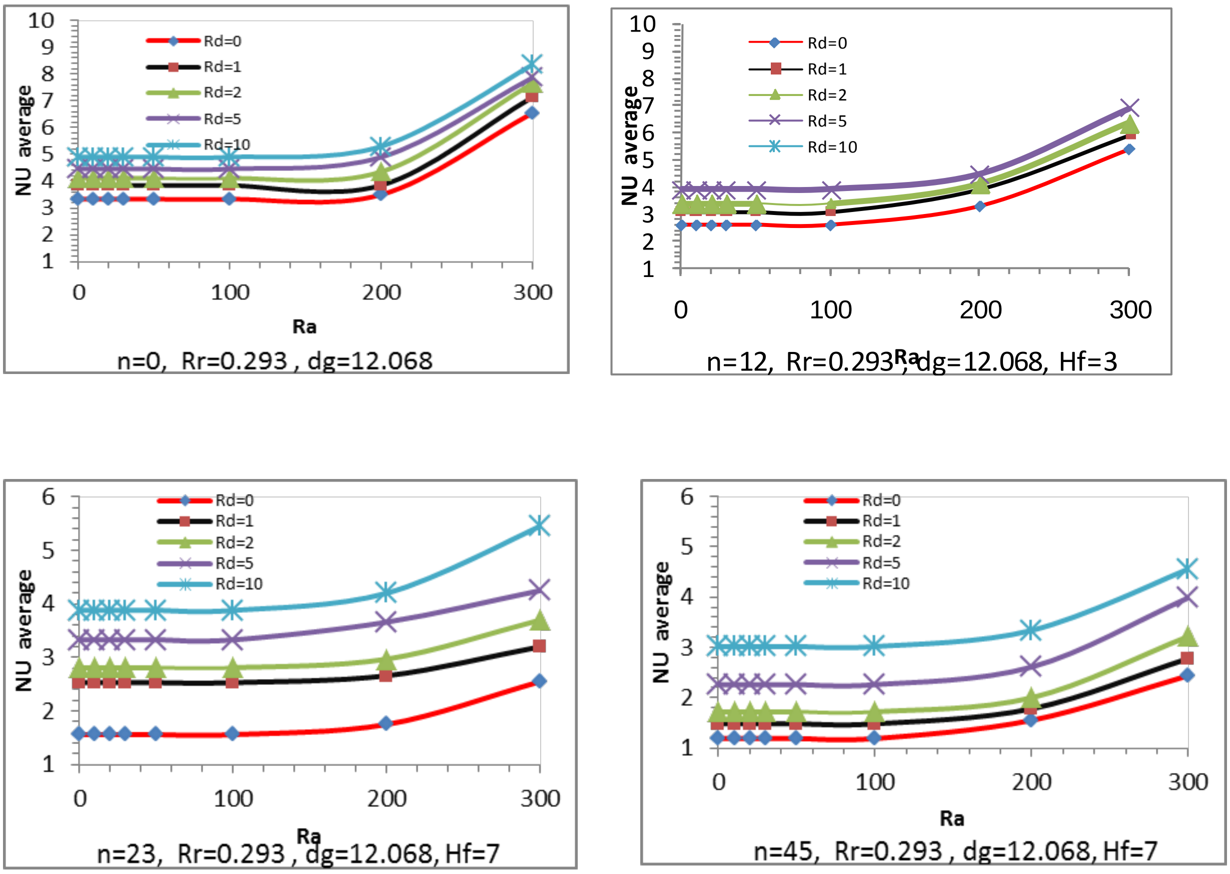

Fig.10 Variation of Average Nu with Ra with different Rd

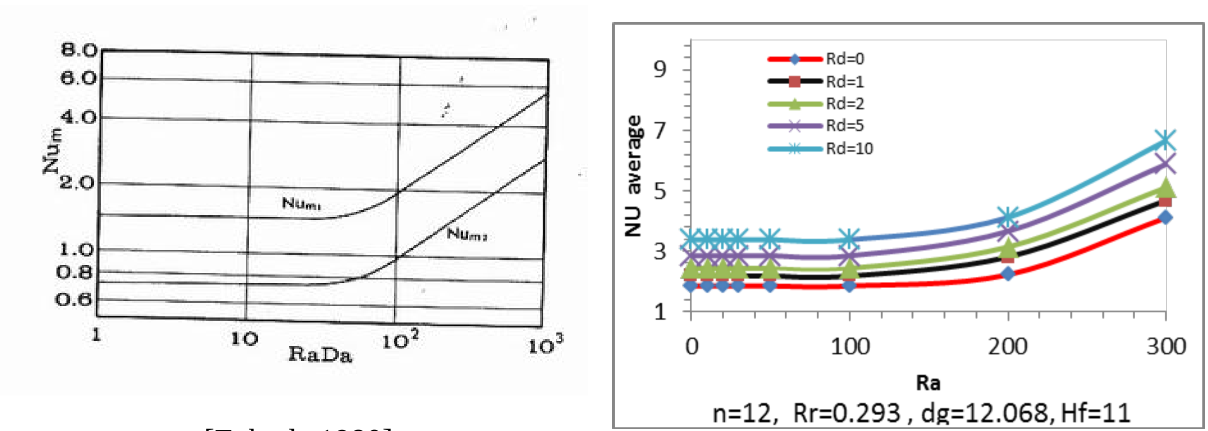

[Fukuda 1980]

Present work

Fig.11 Variation of Average Nusselt number with Modified Rayleigh Number for theoretical part

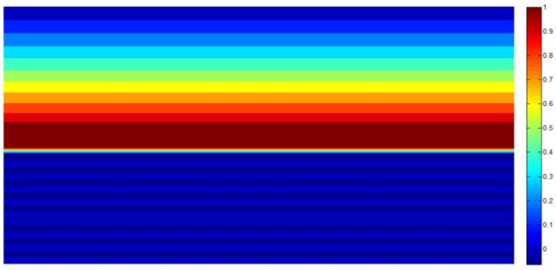

n=0 Rd=0 Ra=100 Rr=0.293 d_g=12.068

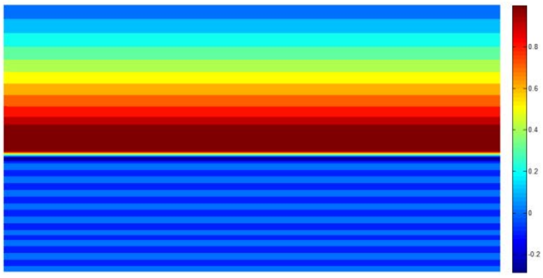

n=0 Rd=5 Ra=100 Rr=0.293 d_g=12.068

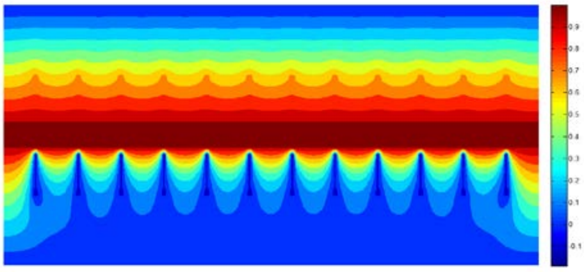

n=12 Rd=0 Ra=100 Rr=0.293 d_g=12.068 Hf=7

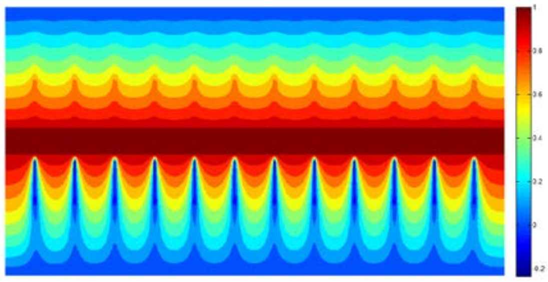

n=12 Rd=5 Ra=100 Rr=0.293 d_g=12.068 Hf=7

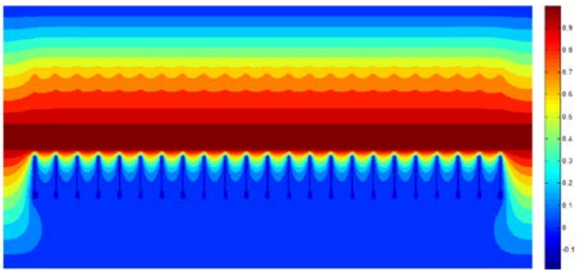

n=23 Rd=0 Ra=100 Rr=0.293, d_g=12.068 Hf=7

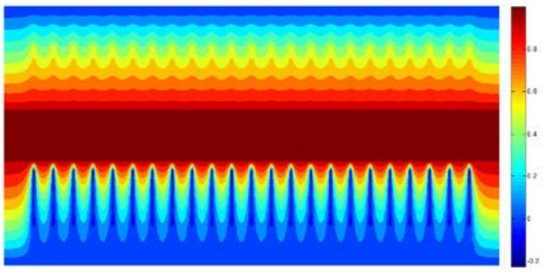

n=23 Rd=5 Ra=100 Rr=0.293, d_g=12.068mm Hf=7

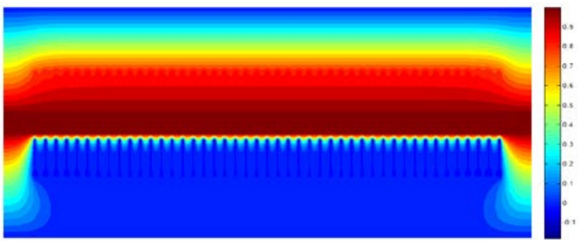

n=45 Rd=0 Ra=100 Rr=0.293 d_g=12.068 Hf=7

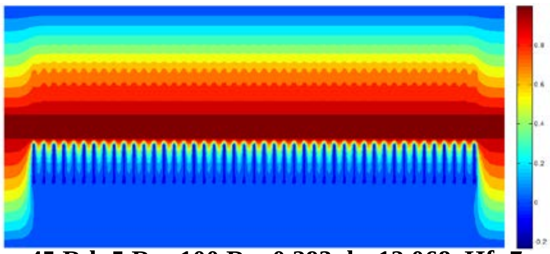

n=45 Rd=5 Ra=100 Rr=0.293 d_g=12.068 Hf=7

Fig.12 Temperature Distribution

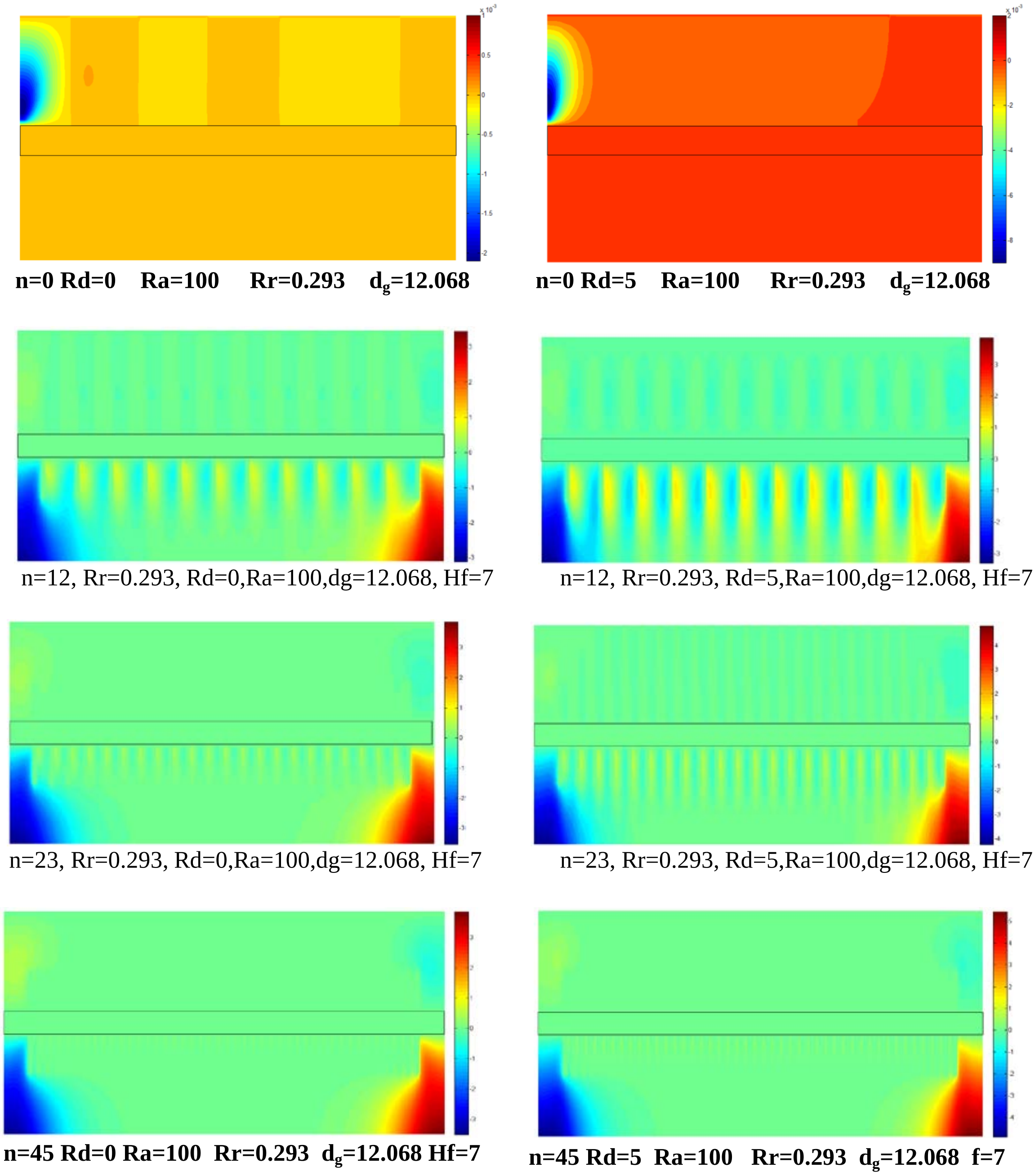

Fig.13 contours of streamline

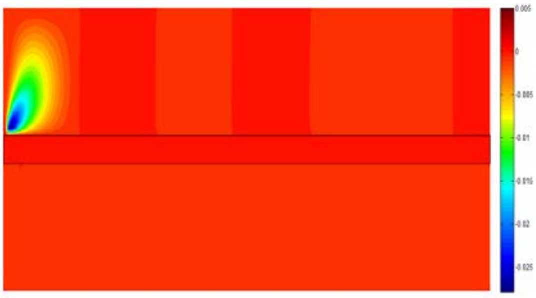

n=0 Rd=0 Ra=100 Rr=0.293 d_g=12.068 mm

n=0 Rd=5 Ra=100 Rr=0.293 d_g=12.068 mm

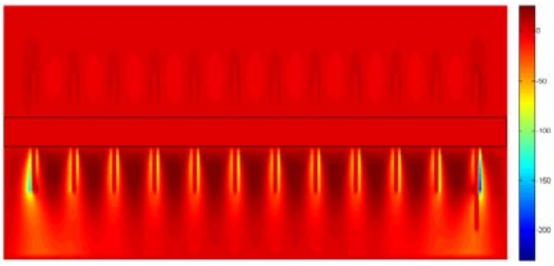

n=12 Rd=0 Ra=100 Rr=0.293 d_g=12.068 Hf=7

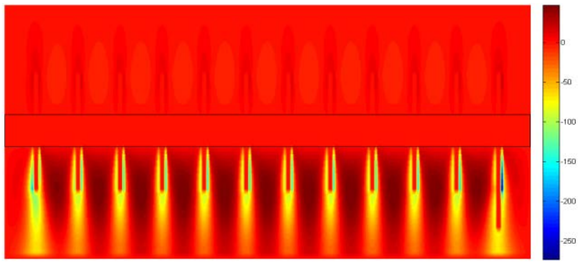

n=12 Rd=5 Ra=100 Rr=0.293d_g=12.068 Hf=7

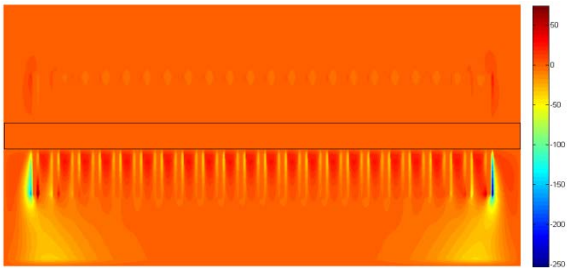

n=23 Rd=0 Ra=100 Rr=0.293 d_g=12.068 Hf=7

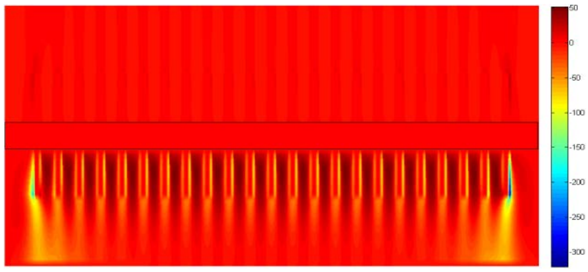

n=23 Rd=5 Ra=100 Rr=0.293 d_g=12.068 Hf=7

n=45 Rd=0 Ra=100 Rr=0.293 d_g=12.068 Hf=7

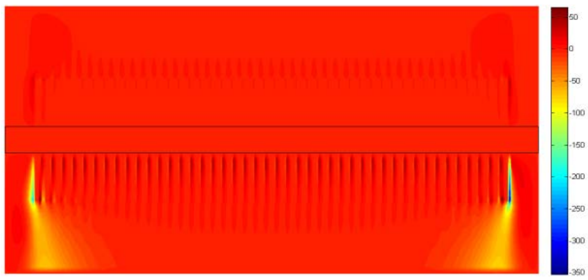

n=45 Rd=5 Ra=100 Rr=0.293 d_g=12.068 Hf=7

Fig.14 Velocity Field Ur

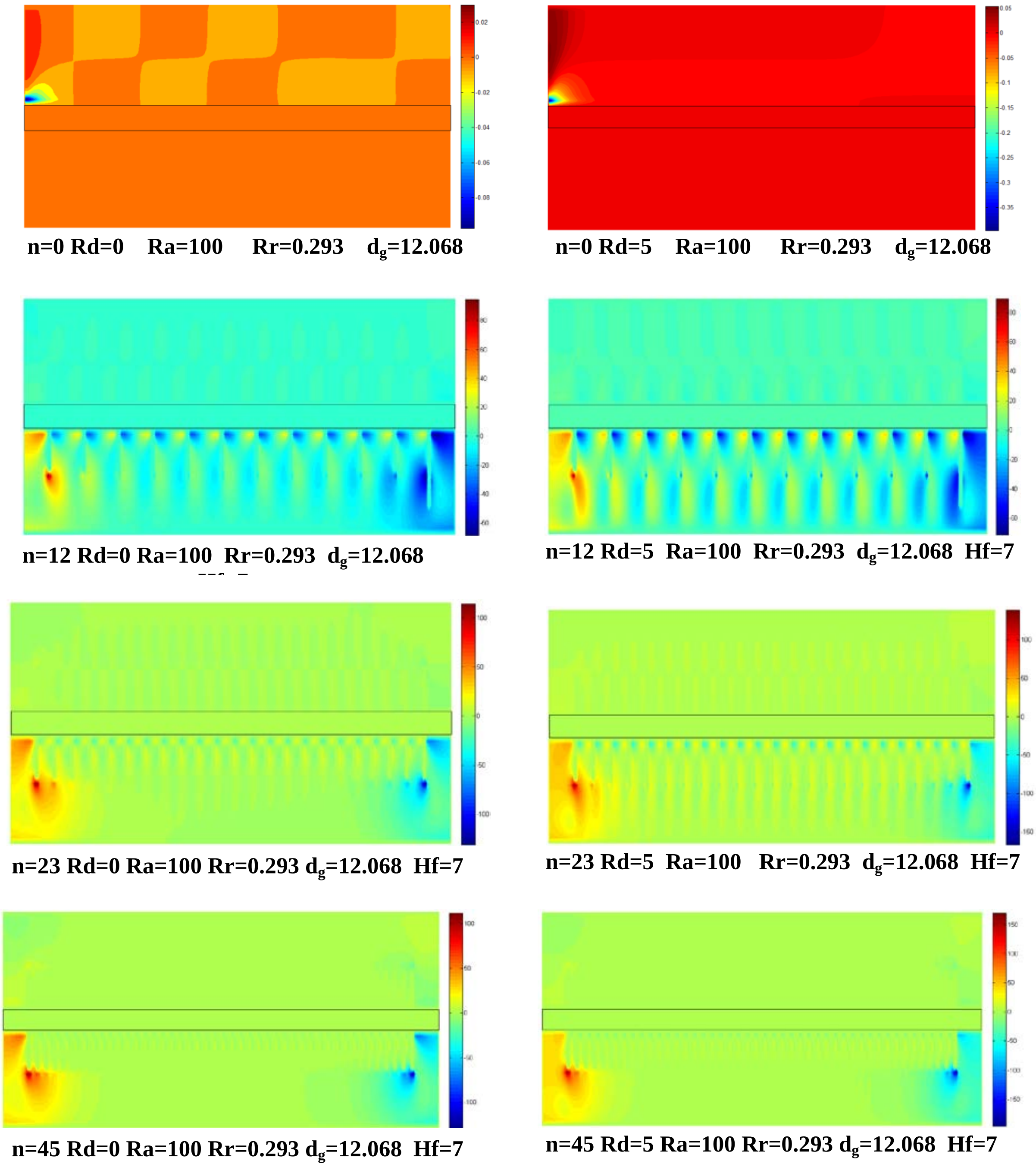

Fig.15 Velocity Field Uz

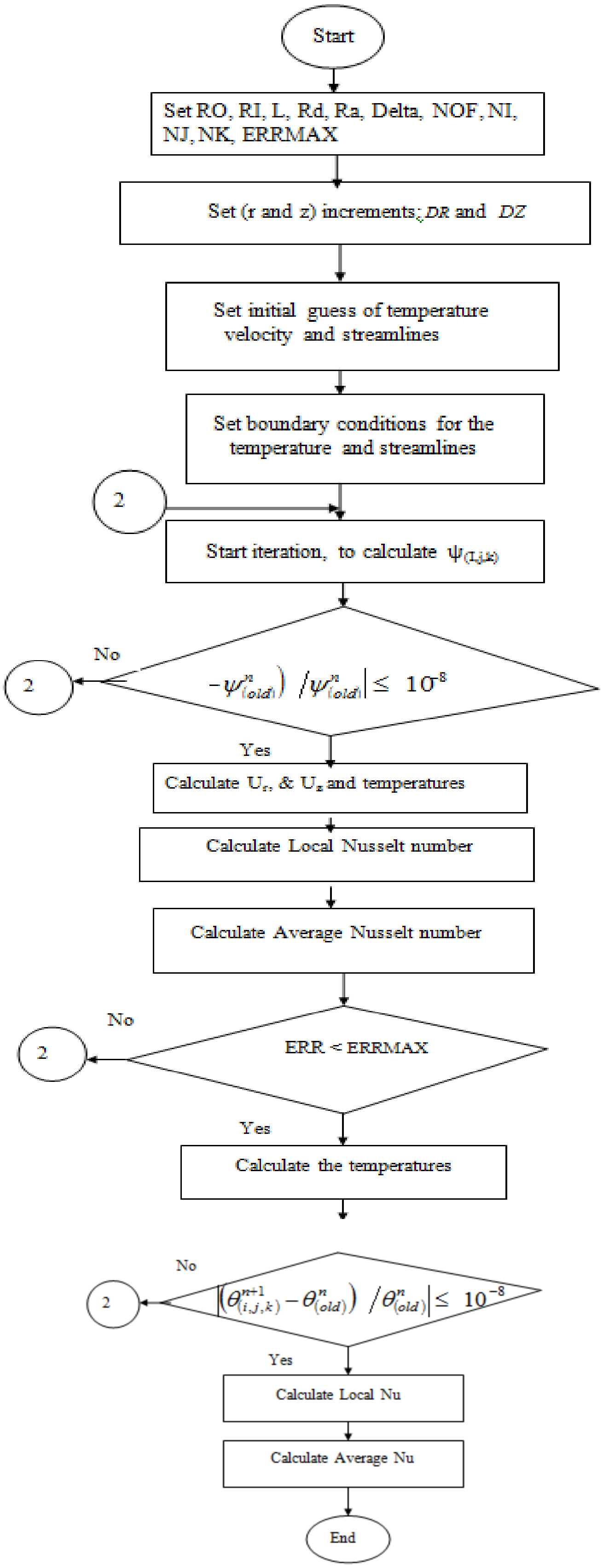

Fig. 16 Flow chart for computer program